ISSN 1674-1056
http://cpb.iphy.ac.cn
http://iopscience.iop.org/cpb
中国物理 B
Chinese Physics
中国物理
Chinese Physics B

# Dynamic characteristics in an external-cavity multi-quantum-well laser

Sen-Lin Yan(颜森林)
**Citation:**Chin. Phys. B . 2018, 27(6): 060501. **doi:** 10.1088/1674-1056/27/6/060501

Journal homepage: http://cpb.iphy.ac.cn; http://iopscience.iop.org/cpb

**What follows is a list of articles you may be interested in**

---

## Stochastic bifurcations of generalized Duffing-van der Pol system with fractional derivative under colored noise

Wei Li(李伟), Mei-Ting Zhang(张美婷), Jun-Feng Zhao(赵俊锋)
Chin. Phys. B . 2017, 26(9): 090501. **doi:** 10.1088/1674-1056/26/9/090501

## Bifurcation and chaos in high-frequency peak current mode Buck converter

Chang-Yuan Chang(常昌远), Xin Zhao(赵欣), Fan Yang(杨帆), Cheng-En Wu(吴承恩)
Chin. Phys. B . 2016, 25(7): 070504. **doi:** 10.1088/1674-1056/25/7/070504

## Bursting phenomena as well as the bifurcation mechanism in a coupled BVP oscillator with periodic excitation

Xiaofang Zhang(张晓芳), Lei Wu(吴磊), Qinsheng Bi(毕勤胜)
Chin. Phys. B . 2016, 25(7): 070501. **doi:** 10.1088/1674-1056/25/7/070501

## A new piecewise linear Chen system of fractional-order: Numerical approximation of stable attractors

Marius-F. Danca, M. A. Aziz-Alaoui, Michael Small
Chin. Phys. B . 2015, 24(6): 060507. **doi:** 10.1088/1674-1056/24/6/060507

## Bifurcation behavior and coexisting motions in a time-delayed power system

Ma Mei-Ling, Min Fu-Hong
Chin. Phys. B . 2015, 24(3): 030501. **doi:** 10.1088/1674-1056/24/3/030501

---

# Dynamic characteristics in an external-cavity multi-quantum-well laser

Sen-Lin Yan(颜森林)†

*Department of Electronic Engineering, Nanjing Xiaozhuang University, Nanjing* 211171, *China*

(Received 20 February 2018; revised manuscript received 23 March 2018; published online 10 May 2018)

This paper outlines our studies of bifurcation, quasi-periodic road to chaos and other dynamic characteristics in an external-cavity multi-quantum-well laser with delay optical feedback. The bistable state of the laser is predicted by finding theoretically that the gain shifts abruptly between two values due to the feedback. We make a linear stability analysis of the dynamic behavior of the laser. We predict the stability scenario by using the characteristic equation while we make an approximate analysis of the stability of the equilibrium point and discuss the quantitative criteria of bifurcation. We deduce a formula for the relaxation oscillation frequency and prove theoretically that this formula function relates to the loss of carriers transferring between well regime and barrier regime, the feedback level, the delayed time and the other intrinsic parameters. We demonstrate the dynamic distribution and double relaxation oscillation frequency abruptly changing in periodic states and find the multi-frequency characteristic in a chaotic state. We illustrate a road to chaos from a stable state to quasi-periodic states by increasing the feedback level. The effects of the transfers of carriers and the escaping of carriers on dynamic behavior are analyzed, showing that they are contrary to each other via the bifurcation diagram. Also, we show another road to chaos after bifurcation through changing the linewidth enhancement factor, the photon loss rate and the transfer rate of carriers.

**Keywords:** bifurcation, chaos, multi-quantum-well laser, optical feedback

**PACS:** 05.45.–a, 05.45.Pq, 02.30.Ks, 02.30.Oz **DOI:** 10.1088/1674-1056/27/6/060501

## 1. Introduction

Optical chaos is one kind of ubiquitous nonlinear optic phenomenon. Chaos is very sensitive to its initial condition while its long-term behavior is difficult to predict.[1–5] A chaotic signal generated by a laser has the advantages of high frequency and large broadband. There were extensive studies of many kinds of chaotic lasers and their applications in secure communication,[6–9] including the vertical-cavity surface-emitting laser, multi-mode solid Nd:YAG laser, erbium-doped fiber laser and others.[10–15] Optical feedback or injection semiconductor lasers can readily emit optical chaotic signals.[16–21] They are easily manufactured, and are preferred to be used as carrier transmitters in chaotic laser applications. The studies of the frequency characteristic and dynamics behavior in an external cavity semiconductor laser were recently highlighted because they are significant both in physical aspect and in application, such as bistable devices for optical flip-flops, high-frequency generation for optical clocks, or secure communication with a chaotic carrier.[16–21]

Many researchers are very interested in the dynamics in a semiconductor laser with optical feedback since it is an excellent model for nonlinear optical systems and shows many kinds of dynamic behaviors, such as stable state, periodic and quasi-periodic oscillations, and chaos.[3] The dynamic behaviors of external-cavity semiconductor lasers have been extensively studied. However, very little work has been done on dynamics in multiple-quantum-well (MQW) laser with an external cavity. There are carriers from the barrier region to the well layer in a MQW laser, so the MQW laser has more complexity and it is more difficult in theory than a semiconductor laser. We find that the transfers of carriers can remarkably change the laser dynamics. This study of the MQW laser possesses the reference value to complex systems, chaotic dynamics and laser physics.[22–30]

The main objective of this paper is to describe how the laser develops a road to chaos after bifurcation as a function of the feedback level, delayed time and the transfers of carriers. We believe that the abrupt change of the gain can lead to a bistable state and dual-frequency for the periodic state in the MQW laser due to the feedback. We study the stability of the system by discussing the characteristic equation and make some approximate analyses of the stability of the equilibrium point to analyze the quantitative criteria of bifurcation. We present other roads to chaos after bifurcation by changing the linewidth enhancement factor, the photon loss rate and the carrier loss rate.

## 2. Theoretical model

An external cavity semiconductor laser with optical delay feedback shows many complex dynamical behaviors, such as bifurcation and chaos.[13–18] A road to chaos after bifurcation was also investigated with the feedback levels. In this paper, we study the frequency characteristics and dynamic behaviors in an external-cavity separate confinement heterostructure (SCH) MQW laser with optical delay feedback be-

†Corresponding author. E-mail: senlinyan@163.com

© 2018 Chinese Physical Society and IOP Publishing Ltd 

cause MQW laser is widely used in optical communication and other areas. Figure 1 gives a schematic diagram of the external-cavity MQW laser. Considering the optical delay feedback, carriers transferring from the barrier region to the well layer and escaping from the well region to the SCH layer, the dynamics of the external-cavity MQW laser is described by the following equations[7–15]

$$\begin{aligned}\frac{\mathrm{d}E}{\mathrm{d}t} &= \frac{1}{2}(G-\gamma_\mathrm{p})E(t)+\frac{k}{\tau_l}E(t-\tau)\\ &\quad\times\cos\left[\varphi(t)-\varphi(t-\tau)+\omega\tau\right], \qquad (1a)\\ \frac{\mathrm{d}\varphi}{\mathrm{d}t} &= \frac{1}{2}\beta_\mathrm{c}(G-\gamma_\mathrm{p})-\frac{k}{\tau_l}\frac{E(t-\tau)}{E(t)}\\ &\quad\times\sin\left[\varphi(t)-\varphi(t-\tau)+\omega\tau\right], \qquad (1b)\\ \frac{\mathrm{d}N_B}{\mathrm{d}t} &= \eta_\mathrm{i}\frac{I}{q}-\gamma_\mathrm{BQ}N_B+\gamma_\mathrm{QB}N, \qquad (1c)\\ \frac{\mathrm{d}N}{\mathrm{d}t} &= \gamma_\mathrm{BQ}N_B-(\gamma_\mathrm{e}+\gamma_\mathrm{QB})N-GV_\mathrm{p}E^2, \qquad (1d)\end{aligned}$$

where $E$ and $\varphi$ denote the amplitude and phase of the optical field, $N_\mathrm{B}$ and $N$ represent the carriers in the barrier region and in the well region, respectively. The nonlinear mode gain is

$$G=[(\Gamma g_0 v_\mathrm{g})/(1+E^2/E_\mathrm{s}^2)]\times\lg\{(N+N_\mathrm{s})/(N_\mathrm{th}+N_\mathrm{s})\},$$

where $g_0$ is the gain constant; $\Gamma=V/V_\mathrm{p}$ is the mode confinement coefficient with $V$ being the volume of laser cavity and $V_\mathrm{p}$ being the mode volume of laser; $v_\mathrm{g}$ is the group velocity of photons in the laser cavity; $E_\mathrm{s}=(P_\mathrm{s}/V_\mathrm{p})^{1/2}$ is the amplitude of the optical field at saturation with saturation photon number $P_\mathrm{s}$; $N_\mathrm{s}=n_\mathrm{s}V$ is the carrier number, with $n_\mathrm{s}$ being the density of carriers at photon saturation; $N_\mathrm{th}=n_\mathrm{th}V$ is the carrier number at transparency with $n_\mathrm{th}$ being the density of carriers. The $\gamma_\mathrm{p}=(\alpha_\mathrm{m}+\alpha_\mathrm{int})$ is the total photon loss for the group velocity $v_\mathrm{g}$, which is the sum of the cavity loss ($\alpha_\mathrm{m}$) and the internal loss ($\alpha_\mathrm{int}$). The $\beta_\mathrm{c}$ is the optical linewidth enhancement factor. The $\tau_l=2n_\mathrm{g}l/c$ is the round-trip time in the cavity with length $l$, with $c$ being the light velocity in a vacuum, and $n_\mathrm{g}=c/v_\mathrm{g}$ being the group refractive index. The $\eta_\mathrm{i}$ is the internal quantum efficiency, $I$ the drive current, $q$ the unit charge, $\gamma_\mathrm{BQ}$ the loss of carriers from the barrier region to the well layer and $\gamma_\mathrm{QB}$ the loss of carriers escaping from the well region to the SCH layer. The $\gamma_\mathrm{e}=A_\mathrm{nr}+B_\mathrm{nr}(N/V)+C_\mathrm{A}(N/V)^2$ is the total carrier loss in the active layer, with $A_\mathrm{nr}$ being the nonradiative recombination rate, $B_\mathrm{nr}$ the radiative recombination coefficient and $C_\mathrm{A}$ the Auger recombination coefficient. The $k$ is the optical feedback factor and $\tau$ is the external cavity round-trip time.

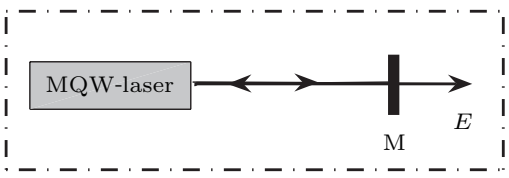



**Fig. 1.** Schematic diagram of external-cavity multi-quantum-well laser. M: half mirror. MQW-laser: the multi-quantum-well laser. $E$: optical field.

### 2.1. Analysis of stable point

Firstly, we analyze the dynamical stability of the laser. Unmoving point $(E_0, N_{\mathrm{B}0}, N_0)$ in Eq. (1) is obtained by

$$\begin{aligned}&(G_0-\gamma_\mathrm{p})+2\rho\cos\omega_0\tau=0, \qquad (2a)\\ &\beta_\mathrm{c}(G_0-\gamma_\mathrm{p})-2\rho\sin\omega_0\tau=0, \qquad (2b)\\ &\eta_\mathrm{i}\frac{I}{q}-\gamma_\mathrm{BQ}N_{\mathrm{B}0}+\gamma_\mathrm{QB}N_0=0, \qquad (2c)\\ &\gamma_\mathrm{BQ}N_{\mathrm{B}0}-(\gamma_{\mathrm{e}0}+\gamma_\mathrm{QB})N_0-G_0V_\mathrm{p}E_0^2=0, \qquad (2d)\end{aligned}$$

where $\rho=k/\tau_l$. From Eqs. (2a) and (2b), we obtain

$$\omega_0\tau=-\tan^{-1}\beta_\mathrm{c}\pm 2n\pi, n\in N, \qquad (3)$$

and

$$G_0=\gamma_\mathrm{p}\pm\frac{2\rho}{\sqrt{1+\beta_\mathrm{c}^2}}. \qquad (4)$$

Variety of nonlinear mode gain is

$$G_{0\mathrm{F}}-G_{0\mathrm{N}}=\pm\frac{2\rho}{\sqrt{1+\beta_\mathrm{c}^2}}, \qquad (5)$$

where $G_{0\mathrm{F}}$ denotes the nonlinear mode gain with the feedback and $G_{0\mathrm{N}}$ represents the nonlinear mode gain without the feedback.

We find that the nonlinear mode gain shifts abruptly around the value $\gamma_\mathrm{p}$ due to the optical feedback, where the abrupt shift is related to the feedback level while the laser results in a bistable state and the laser output is based on the following expression:

$$E_0^2=\frac{\eta_\mathrm{i}\dfrac{I}{q}-\gamma_{\mathrm{e}0}N_0}{\gamma_\mathrm{p}\pm\dfrac{2\rho}{\sqrt{1+\beta_\mathrm{c}^2}}}. \qquad (6)$$

From Eqs. (2c) and (2d), we obtain

$$\eta_\mathrm{i}I/q-\gamma_{\mathrm{e}0}N_0-G_0V_\mathrm{p}E_0^2=0. \qquad (7)$$

We find no effects of the loss of carriers from the barrier region to the well layer and the loss of carriers escaping from the well region to the SCH layer on the stability of the laser. However, their behavior changes the dynamics of the laser.

Secondly, we set the phase stable solution and let $\varphi=\Delta\omega t$, where $\Delta\omega$ is the phase difference from the phase of a stable state. Considering the effect of the external-cavity feedback on the phase, we can rewrite Eq. (2b) as

$$\beta_\mathrm{c}(G_0-\gamma_\mathrm{p})-2\rho\sin\omega_0\tau=\Delta\omega. \qquad (8)$$

We obtain

$$G_0=\gamma_\mathrm{p}\pm\frac{\sqrt{4\rho^2+4\rho\Delta\omega\cos\omega_0\tau+(\Delta\omega)^2}}{\sqrt{1+\beta_\mathrm{c}^2}}, \qquad (9)$$

where

$$\omega_0\tau = -\arcsin\left(\Delta\omega/\sqrt{1+\beta_c^2}\right) - \arctan\beta_c,$$

or

$$\Delta\omega = -\rho\sqrt{1+\beta_c^2}\sin\left(\omega_0\tau + \arctan\beta_c\right). \tag{10}$$

Variety of the nonlinear mode gain is

$$G_{0F} - G_{0N} = \pm\frac{\sqrt{4\rho^2 + 4\rho\Delta\omega\cos\omega_0\tau + (\Delta\omega)^2}}{\sqrt{1+\beta_c^2}}. \tag{11}$$

The maximum value of nonlinear mode gain is

$$G_{0\max} = \gamma_p + \frac{2\rho + \Delta\omega}{\sqrt{1+\beta_c^2}}. \tag{12a}$$

The minimum value of nonlinear mode gain is

$$G_{0\min} = \gamma_p - \frac{2\rho + \Delta\omega}{\sqrt{1+\beta_c^2}}. \tag{12b}$$

The nonlinear mode gain shifts between $G_{0\max}$ and $G_{0\min}$. The laser output shifts between two levels, based on the following expression:

$$E_0^2 = \frac{\eta_i\dfrac{I}{q} - \gamma_{e0}N_0}{\gamma_p \pm \dfrac{\sqrt{4\rho^2 + 4\rho\Delta\omega\cos\omega_0\tau + (\Delta\omega)^2}}{\sqrt{1+\beta_c^2}}}. \tag{13}$$

Equation (11) predicts the bistable state produced by the feedback, again.

### 2.2. Analysis of stability

To evaluate the stability, dynamics and frequency characteristics of the laser mode, a small signal perturbation analysis is implemented via the linear stability theory. We assume a small perturbation from the laser stationary position to excite the system to oscillation around its stable position ($E_0$, $\varphi_0$, $N_{B0}$, $N_0$). The laser mode may become rapidly unstable because of the abrupt change of the gain. The following approximations are adopted:

$$E(t) = E_0 + \delta E\,\mathrm{e}^{\lambda t}, \quad \varphi(t) = \varphi_0 + \delta\varphi\,\mathrm{e}^{\lambda t},$$
$$N_B(t) = N_{B0} + \delta N_B\,\mathrm{e}^{\lambda t}, \quad N(t) = N_0 + \delta N\,\mathrm{e}^{\lambda t},$$

where $\lambda$ is assumed to be a characteristic value, and

$$G(N_0+\delta N,\, E_0+\delta E) = G_0(N_0, E_0) + G_N\delta N + G_E\delta E,$$
$$\gamma_e(N_0+\delta N) = \gamma_{e0}(N_0) + \gamma_{e0}\delta N,$$
$$G_E = \frac{\partial G}{\partial E}\Big|_{N=N_0,E=E_0} = (\Gamma g_0 v_g)\frac{-2E_0/E_s^2}{(1+E_0^2/E_s^2)^2}\lg\frac{N_0+N_s}{N_{th}+N_s},$$
$$G_N = \frac{\partial G}{\partial N}\Big|_{N=N_0,E=E_0} = (\Gamma g_0 v_g)\frac{1}{(1+E_0^2/E_s^2)}\frac{1}{N_0+N_s},$$

$$\gamma_{eN} = \frac{\partial\gamma_e}{\partial N}\Big|_{N=N_0} = \frac{B_{nr}}{V} + 2C_A\frac{N_0}{V^2}.$$

We substitute them into Eq. (1), and the linearzation of the system (1) will be able to be written by a perturbation equation as follows:

$$\frac{\mathrm{d}}{\mathrm{d}t}\begin{pmatrix}\delta E\\ \delta\varphi\\ \delta N_B\\ \delta N\end{pmatrix} = \begin{pmatrix}A_{11} & A_{12} & A_{13} & A_{13}\\ A_{21} & A_{22} & A_{23} & A_{23}\\ A_{31} & A_{32} & A_{33} & A_{34}\\ A_{41} & A_{42} & A_{43} & A_{44}\end{pmatrix}\begin{pmatrix}\delta E\\ \delta\varphi\\ \delta N_B\\ \delta N\end{pmatrix}, \tag{14}$$

where

$$A_{11} = \frac{1}{2}E_0G_E + \frac{k}{\tau_l}(\mathrm{e}^{-\lambda\tau}-1)\cos(\omega_0\tau),$$
$$A_{12} = \frac{k}{\tau_l}(\mathrm{e}^{-\lambda\tau}-1)E_0\sin(\omega_0\tau),$$
$$A_{13} = 0,$$
$$A_{14} = \frac{1}{2}E_0G_N,$$
$$A_{21} = \frac{1}{2}\beta_cG_E - \frac{k}{\tau_l}\frac{1}{E_0}(\mathrm{e}^{-\lambda\tau}-1)\sin(\omega_0\tau),$$
$$A_{22} = \frac{k}{\tau_l}(\mathrm{e}^{-\lambda\tau}-1)\cos(\omega_0\tau),$$
$$A_{23} = 0,$$
$$A_{24} = \frac{1}{2}\beta_cG_N,$$
$$A_{31} = 0,$$
$$A_{32} = 0,$$
$$A_{33} = -\gamma_{BQ},$$
$$A_{34} = \gamma_{QB},$$
$$A_{41} = -2G_0V_pE_0 - V_pE_0^2G_E,$$
$$A_{42} = 0,$$
$$A_{43} = \gamma_{BQ},$$
$$A_{44} = -\gamma_{e0} - \gamma_{QB} - N_0\gamma_{eN} - V_pE_0^2G_N,$$

whose associated characteristic equation is obtained from

$$\lambda^4 + \lambda^3 b_{s1} + \lambda^2 b_{s2} + \lambda b_{s3} + b_{s4} = 0, \tag{15}$$

with

$$\begin{aligned}
b_{s1} &= -(A_{11}+A_{22}+A_{33}+A_{44}),\\
b_{s2} &= (A_{11}A_{44} - A_{12}A_{21} - A_{34}A_{43} + A_{22}A_{33} + A_{33}A_{44}\\
&\quad + A_{11}A_{22} + A_{22}A_{44} + A_{11}A_{33} - A_{41}A_{14}),\\
b_{s3} &= (A_{21}A_{12}A_{33} + A_{21}A_{12}A_{44} - A_{11}A_{22}A_{44} - A_{11}A_{33}A_{44}\\
&\quad + A_{11}A_{34}A_{43} - A_{22}A_{33}A_{44} + A_{22}A_{34}A_{43} + A_{41}A_{14}A_{33}\\
&\quad - A_{41}A_{12}A_{14} + A_{41}A_{22}A_{14} - A_{11}A_{22}A_{33}),\\
b_{s4} &= (A_{11}A_{22}A_{33}A_{44} - A_{11}A_{22}A_{34}A_{43} - A_{21}A_{12}A_{33}A_{44}\\
&\quad + A_{21}A_{12}A_{34}A_{43} - A_{41}A_{12}A_{24}A_{33} - A_{41}A_{22}A_{14}A_{33}).
\end{aligned}$$

Let

$$\rho = k/\tau, \quad a_{11} = E_0G_E/2, \quad a_{21} = \beta_cG_E/2,$$

$$
\begin{aligned}
b_{11} &= (a_{11}+A_{33}+A_{44}), \quad b_{12} = -2\rho\cos\omega_0\tau,\\
b_{21} &= (a_{11}A_{44}-A_{34}A_{43}+A_{33}A_{44}-A_{41}A_{14}+a_{11}A_{33}),\\
b_{22} &= -\rho\cos\omega_0\tau(2A_{44}+2A_{33}+a_{11})+a_{21}\rho E_0\sin\omega_0\tau,\\
b_{31} &= -a_{11}(A_{33}A_{44}-A_{34}A_{43})+A_{41}A_{14}A_{33},\\
b_{32} &= [-a_{21}(A_{33}+A_{44})+A_{41}A_{14}]\rho E_0\sin\omega_0\tau\\
&\quad +[a_{11}(A_{44}+A_{33})+2\rho(A_{33}A_{44}+A_{34}A_{43})\\
&\quad -A_{41}A_{14}]\rho\cos\omega_0\tau,\\
b_{33} &= -\rho^2(A_{33}+A_{44}),\\
b_{42} &= [-a_{11}(A_{33}A_{44}-A_{34}A_{43})+A_{41}A_{14}A_{33}]\rho\cos\omega_0\tau\\
&\quad +[a_{21}(A_{33}A_{44}-A_{34}A_{43})+A_{41}A_{24}A_{33}]\rho E_0\sin\omega_0\tau,\\
b_{44} &= \rho^2[A_{33}A_{44}-A_{34}A_{43}],
\end{aligned}
$$

and we will obtain a characteristic equation as follows:

$$
\begin{aligned}
&\lambda^4-\lambda^3[b_{11}+b_{12}(1-\mathrm{e}^{-\lambda\tau})]\\
&+\lambda^2[b_{21}+b_{22}(1-\mathrm{e}^{-\lambda\tau})+\rho^2(1-\mathrm{e}^{-\lambda\tau})^2]\\
&+\lambda[b_{31}+b_{32}(1-\mathrm{e}^{-\lambda\tau})+b_{33}(1-\mathrm{e}^{-\lambda\tau})^2]\\
&+b_{42}(1-\mathrm{e}^{-\lambda\tau})+b_{44}(1-\mathrm{e}^{-\lambda\tau})^2=0. \qquad (16)
\end{aligned}
$$

Equation (16) is a transcendental equation and has no analytical solution while it is very difficult to obtain the numerical solutions but with zero root. However, we may predict the stability of the system or make some approximate analyses of the stability.

Firstly, we predict generally the stability as follows.

(i) If the real part of one of the roots of Eq. (16) has a positive value, the equilibrium point of the system will be unstable.

(ii) If all real parts of the roots of Eq. (16) are negative values, the equilibrium point of the system will be asymptotically stable.

(iii) If the root of Eq. (16) has a pair of purely imaginary numbers and the others are negative, it may imply that bifurcation will occurs in the laser while bifurcation processes will happen in different delayed time regions.

Secondly, we will give a simplified equation to conduct the approximate analysis of the stability. When a small region of the current is set to be above the threshold, we expect that the dynamic in the system is determined by the eigenfrequencies of the laser and assume that all roots of Eq. (16) have the real part values, and let $\exp(-\lambda\tau)\approx 1-\lambda\tau+(\lambda\tau)^2/2$. Inserting these assumptions into Eq. (16), we obtain a simplified characteristic equation for the eigen values to the second order approximation as follows:

$$\lambda^4+\lambda^3 b_1+\lambda^2 b_2+\lambda b_3+b_4=0, \qquad (17)$$

where

$$
\begin{aligned}
b_1 &= 2(1-b_{12}\tau-b_{22}\tau^2/2+\rho^2\tau^2)/b_{12}\tau^2,\\
b_2 &= 2(b_{33}\tau^2-b_{11}+b_{22}\tau-b_{32}\tau^2)/b_{12}\tau^2,\\
b_3 &= 2(b_{21}+b_{32}\tau-b_{42}\tau^2/2+b_{44}\tau^2)/b_{12}\tau^2,\\
b_4 &= 2(b_{31}+\tau b_{42})/b_{12}\tau^2.
\end{aligned}
$$

We obtain the following results.

i) When $b_1>0$, $b_4>0$, $b_1\times b_2-b_3>0$, real parts of all roots of Eq. (17) are the negative values, the equilibrium point of the system will be stable.

ii) When $b_1<0$, or $b_4<0$, or $b_1\times b_2-b_3<0$, real parts of all roots of Eq. (17) are the positive values, the equilibrium point of the system will be unstable.

Let $\lambda=u-b_1/4$ to simplify Eq. (17) to understand the unstable point characteristic, we obtain

$$u^4+au^2+bu+cu=0, \qquad (18)$$

where

$$
\begin{aligned}
a &= -\frac{3}{8}b_1^2+b_2,\\
b &= \frac{1}{8}b_1^3-\frac{1}{2}b_1b_2+b_3,\\
c &= -\frac{3}{4^4}b_1^4+\frac{1}{16}b_1^2b_2+b_4.
\end{aligned}
$$

We obtain

$$u^2+\frac{1\pm\sqrt{8y_0+1-4a}}{2}u+\left(y_o\pm\frac{y_0-b}{\sqrt{8y_0+1-4a}}\right)=0, \qquad (19)$$

where $y_0$ is a real root that is determined by

$$y^3-\frac{a}{2}y^2+\frac{b-4c}{4}y+\frac{c(4a-1)-b^2}{8}=0. \qquad (20)$$

Let

$$
\begin{aligned}
B_\pm &= \frac{1\pm\sqrt{8y_0+1-4a}}{2},\\
C_\pm &= y_o\pm\frac{y_0-b}{\sqrt{8y_0+1-4a}},
\end{aligned}
$$

and we will obtain

$$u^2+B_\pm u+C_\pm=0. \qquad (21)$$

We obtain

$$u=\frac{-B_\pm\pm\sqrt{B_\pm^2-4C_\pm}}{2} \qquad (22)$$

and

$$\lambda=u-\frac{b_1}{4}=\frac{-B_\pm\pm\sqrt{B_\pm^2-4C_\pm}}{2}-\frac{b_1}{4}. \qquad (23)$$

We obtain the following results.

When $B_\pm^2-4C_\pm<0$ and $2B_\pm+2b_1=0$, Hopf bifurcation will occur.

Finally, we assume that $\lambda = \mathrm{j}\xi$ is the root of Eq. (15), only when $\xi$ satisfies

$$\begin{aligned}&\xi^4 - \xi^3 b_{12}\sin\xi\tau\\&-\xi^2[b_{21}+b_{22}(1-\cos\xi\tau)+\rho^2(1-2\cos\xi\tau+\cos2\xi\tau)]\\&+\xi[-b_{32}\sin\xi\tau-b_{33}(2\sin\xi\tau-\sin2\xi\tau)]\\&+b_{42}(1-2\cos\xi\tau)+b_{44}(1-\cos2\xi\tau)=0,\end{aligned}\tag{24a}$$

and

$$\begin{aligned}&\xi^3[b_{11}+b_{12}(1-\cos\xi\tau)]\\&-\xi^2[b_{22}\sin\xi\tau-\rho^2(\sin2\xi\tau-2\sin\xi\tau)]\\&+\xi[b_{31}+b_{32}(1-\cos\xi\tau)+b_{33}(1-2\cos\xi\tau+\cos2\xi\tau)]\\&+b_{42}\sin\xi\tau+b_{44}(2\sin\xi\tau-\sin2\xi\tau)=0,\end{aligned}\tag{24b}$$

equations (24a) and (24b) are still transcendental equations and have no analytical solution while it is also difficult to obtain the numerical solutions.

We will make the approximate analysis of the stability. When the eigenfrequencies are determined based on dynamics of the system, the value $\tau$ is appropriated for the result in $\xi\tau \approx 2n\pi$ ($n \in N$), equation (24) is simplified into

$$\xi^4 - \xi^2 b_{21} - b_{42} = 0, \tag{25a}$$

$$\xi^2 b_{11} + b_{31} = 0. \tag{25b}$$

When the system satisfies the following condition:

$$-\frac{b_{31}}{b_{11}} = \frac{b_{21} \pm \sqrt{b_{21}^2 + 4b_{42}}}{2}, \tag{26}$$

Hopf bifurcation will occur. We obtain

$$\xi = \pm\sqrt{-b_{31}/b_{11}}. \tag{27}$$

### 2.3. Stability and frequency characteristic

When the laser is related to the eigenfrequency, we may take $\omega_0\tau \approx 2n\pi$ ($n \in N$). This can be deduced to $\exp(-\lambda\tau) \approx 1-\lambda\tau$ . Let these assumptions be inserted into Eq. (16) and neglect higher order terms, we obtain

$$\lambda^3 + \lambda^2 B_1 + \lambda B_2 + B_3 = 0, \tag{28}$$

where

$$\begin{aligned}B_1 &= (b_{22}\tau - b_{11})/(1-b_{12}\tau),\\B_2 &= (b_{32}\tau + b_{21})/(1-b_{12}\tau),\\B_3 &= (b_{42}\tau + b_{31})/(1-b_{12}\tau).\end{aligned}$$

We can obtain some results as follows.

(I) When $B_1 > 0$, $B_2 > 0$, $B_3 > 0$ and $B_1B_2 - B_3 > 0$, the real parts of all roots of Eq. (28) have the negative values, the equilibrium point of the system will be asymptotically stable.

(II) When $B_1 < 0$, or $B_3 < 0$, the real parts of the roots of Eq. (16) have the positive values, the equilibrium point of the system will be unstable.

(III) When $B_1 > 0$, $B_3 > 0$, and $B_1B_2 - B_3 = 0$, the root of Eq. (16) will have a pair of purely imaginary numbers, namely

$$\Im(\lambda) = \pm\sqrt{(b_{42}\tau + b_{31})/(b_{22}\tau - b_{11})},$$

implying that the bifurcation will occur in the laser.

To obtain the analytical solution of Eq. (28) and discuss the frequency characteristic, let

$$P = \frac{3B_2 - B_1^2}{3}, \quad Q = \frac{2B_1^2 - 9B_1B_2 + 27B_3}{27}$$

and we will obtain

I) $Z = (2Q)^2 + (P/3)^3 > 0$, a real root and two complex roots are obtained:

$$\begin{aligned}&\lambda_1 = U + V, \quad \lambda_2 = -(U+V)/2 + \mathrm{i}(U-V)\sqrt{3}/2,\\&\lambda_3 = -(U+V)/2 - \mathrm{i}(U-V)\sqrt{3}/2,\end{aligned}$$

where

$$U = \sqrt[3]{-\frac{Q}{2} + \sqrt{\frac{Q^2}{4} + \frac{P^3}{27}}}, \quad V = \sqrt[3]{-\frac{Q}{2} - \sqrt{\frac{Q^2}{4} + \frac{P^3}{27}}};$$

II) $(2Q)^2 + (P/3)^3 = 0$, three real roots are obtained:

$$\lambda_1 = 2\sqrt[3]{-2Q}, \quad \lambda_2 = \lambda_3 = -\sqrt[3]{-3Q};$$

III) $(2Q)^2 + (P/3)^3 < 0$, three different roots are obtained:

$$\begin{aligned}\lambda_1 &= 2\sqrt{-3P}\cos(\varphi/3),\\\lambda_2 &= 2\sqrt{-3P}\cos(2\pi/3 + \varphi/3),\\\lambda_2 &= 2\sqrt{-3P}\cos(2\pi/3 + \varphi/3),\end{aligned}$$

where

$$\cos\varphi = 2q/(3P\sqrt{-3P}).$$

Then

a) when $B_3 < 0$, equation (16) has at least one positive root;

b) when $B_3 \geqslant 0$ and $Z \leq 0$, equation (16) has no positive root;

c) when $B_3 \geqslant 0$ and $Z \leq 0$, equation (16) may have a positive root.

For the imaginary part of $\lambda$, an expression relating to the relaxation oscillation frequency of the laser is obtained by

$$\Omega \propto \mathrm{Im}(\lambda) = \pm 3(U-V)/2, \tag{29}$$

where

$$U = \sqrt[3]{-\frac{Q}{2} + \sqrt{\frac{Q^2}{4} + \frac{P^3}{27}}},$$

$$V = \sqrt[3]{-\frac{Q}{2} - \sqrt{\frac{Q^2}{4} + \frac{P^3}{27}}}.$$

The level and delayed time of the feedback enter into the magnitude of the relaxation frequency. We find that the abrupt changes of the gain and light amplitude result in the abrupt change of the relaxation frequency. The laser has variable-frequency characteristics. When $\rho = 0$, the intrinsic frequency of the laser is obtained by

$$\Omega \propto \pm \frac{\sqrt{4b_{21} - (a_{11} + A_{33} + A_{44})^2}}{2}. \tag{30}$$

The intrinsic frequency is a function of the total carrier loss in the active layer, the total photon loss, the current, the loss of carriers from the barrier region to the well layer and the loss of carriers escaping from the well region to the SCH layer. Equation (18) is different from the formula obtained by Fujiwara *et al.* because the structure of a quantum-well laser is different from that of a semiconductor laser.

## 3. Results and discussion

### 3.1. Road to chaos

Evolving from a stable state to chaos after a quasi-period is presented via a road to chaos. The feedback level is taken as a controllable parameter for the laser system. The laser parameter values for the numerical calculations are listed in the following Table 1.

**Table 1.** Laser parameters.

| Symbol | Value | Unit | Symbol | Value | Unit |
|---|---|---|---|---|---|
| $l$ | 1200 | μm | $B_r$ | $1.0\times10^{-10}$ | $cm^3/s$ |
| $V$ | 50.4 | $\mu m^3$ | $C_A$ | $5.0\times10^{-29}$ | $cm^6/s$ |
| $\Gamma$ | 0.045 | | $P_s$ | $2.2\times10^{7}$ | |
| $n_g$ | 3.6 | | $g_0$ | 2700 | $cm^{-1}$ |
| $n_s$ | $0.1\times10^{18}$ | | $I$ | 50 | mA |
| $\alpha_m$ | 11.5 | $cm^{-1}$ | $n_i$ | 0.8 | |
| $\alpha_{int}$ | 20 | $cm^{-1}$ | $\gamma_{BQ}$ | $2.5\times10^{10}$ | $s^{-1}$ |
| $n_{th}$ | $2.1\times10^{18}$ | $cm^{-3}$ | $\gamma_{QB}$ | $5\times10^{9}$ | $s^{-1}$ |
| $A_{nr}$ | $2.5\times10^{8}$ | $s^{-1}$ | $\beta_c$ | 3 | |

The results are summarized in the phase-parametric approach shown in Figs. 2(a) and 2(b). In the bifurcation diagram, the normalized extremes of the peak series of the laser output versus the feedback level are plotted where the delay time is fixed at $\tau = 0.5$ ns and the horizontal coordinate is divided by fifty equal divisions. A set of extremes of the peak series shows various dynamic states versus feedback level. A road to chaos from a stable state through a quasi-period is clearly seen. The laser shows a stable-state at $k$ values between 0 and 0.078. A stable-state ends or a Hopf bifurcation point occurs at $k = 0.078$. Increasing the feedback level from 0.08 to 0.1782, the laser shows the process of bifurcation to a quasi-period. Undamped behaviors appear at $k$ values between 0.1828 and 0.192. The first chaotic region is distributed between 0.192 and 0.238. The undamped behavior passes through 0.2426. The fully developed chaotic region appears at $k$ values higher than 0.2528.

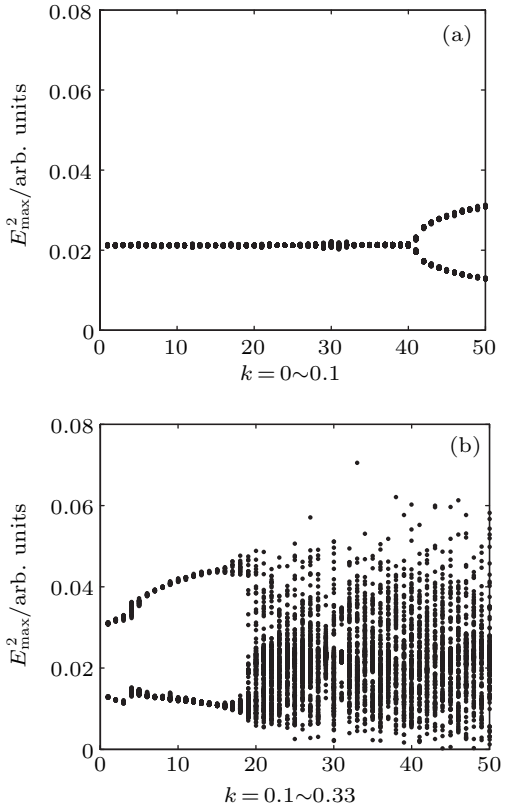



**Fig. 2.** Bifurcation diagram with feedback levels. Vertical axis represents laser output maxima. Horizontal axis denotes feedback level.

### 3.2. Dynamics distribution and relaxation oscillation

We find that the feedback level can cause a significant effect on the dynamics of the laser to form different dynamic regions corresponding to the bifurcation diagram. The relaxation oscillation characteristics of the laser are described in dynamic distribution shown in the bifurcation diagram.

#### 3.2.1. Stable regime

The solitary laser characteristics dominate the behavior of the system. However, we find that it takes a long time for the laser to oscillate after it has become a stable state, with increasing the feedback level. For instance, we find that the laser takes 2.5 ns to perform a damped relaxation oscillation before locking to a stable state when $k = 0.01$ and the laser takes 20 ns to lock to a stable state when $k = 0.07$.

#### 3.2.2. Periodical regime

Within this region, the memory of the first peak of relaxation oscillation begins to control the behavior. The temporal dynamics evolves from undamped relaxation oscillation

to sustained relaxation oscillation and then into a mixed periodic state in which the laser pulses periodically. We find two solitary frequency regimes where the laser abruptly manifests dual-frequency characteristics which appear at the critical point $k = 0.112$. When $k \leq 0.112$, the laser dominates its behavior with relaxation oscillation frequency around 5 GHz; the relaxation oscillation frequency is around 5 GHz shown in Fig. 3 for $k = 0.1$; with increasing the feedback levels, the relaxation oscillation frequency of the laser shifts abruptly while the laser dominates its oscillation behavior around 3.6 GHz as shown in Fig. 4 for $k = 0.15$. This result accords with Eq. (18).

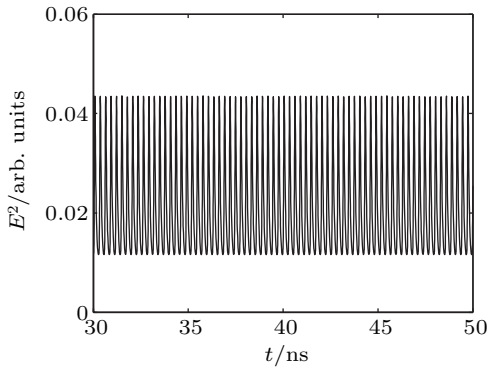



**Fig. 3.** Periodic oscillation around 5 GHz.

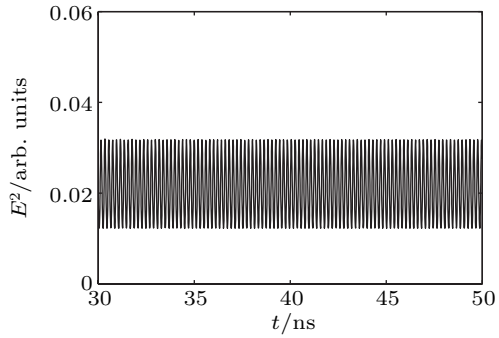



**Fig. 4.** Periodic oscillation around 3.6 GHz.

### 3.2.3. Undamped oscillation regime

In the undamped oscillation region, a small destabilization arises. The periodic initial transient is enhanced by the external cavity and insults in the second transient, which will be recycled by the cavity again and induce another transient and so on. Eventually, the periodic oscillation is ruined. However, the laser ongoing relaxation oscillation has not fully decayed because of the high feedback level, and becomes of the undamped relaxation oscillation.

### 3.2.4. Chaotic regime

With the high feedback levels, the store of the peak of undamped oscillation causes a significant effect on the dynamics behavior. The initial transient is amplified and enchanced by the external cavity and other transients are excited. Subsequent transients become more prolonged until eventually the undamping of the laser turns very sufficient to develop into a chaotic behavior. Each of Figs. 5 and 6 shows the laser output.

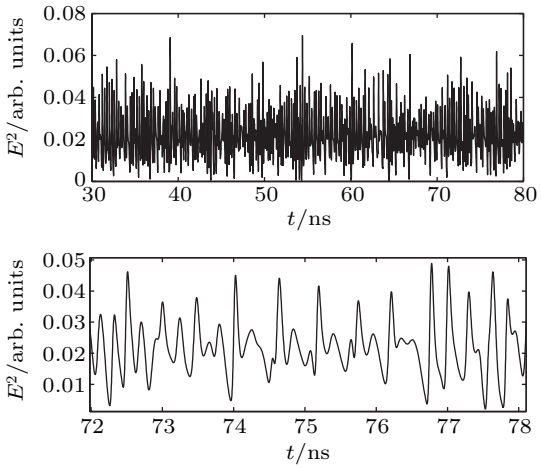



**Fig. 5.** Chaotic oscillation where the lower panel is the zoomed region.

Chaotic oscillation of the laser characterizes frequency expansion or compression found in some time regions. When $k = 0.26$, in Fig. 5 the chaotic oscillation frequencies are around 4.8 GHz between 30 ns and 40 ns, 5.5 GHz between 40 ns and 50 ns,5.3 GHz between 50 ns and 60 ns, 4.6 GHz between 60 ns and 70 ns and 5 GHz between 70 ns and 80 ns, respectively. This varying frequency characterizes a chaotic breathing behavior. The physical mechanism of this phenomenon is that the time-delay-scale with respect to the laser internal timescale and the sensitivity to the phase of feedback field produce a combination of inducing various dynamical scenarios and subsequent oscillations, resulting in the chaotic breathing. Such a breathing variety manifests itself at the feedback level $k = 0.33$ while chaotic relaxation oscillations are around 5.9 GHz between 30 ns and 40 ns, 5.7 GHz between 50 ns and 60 ns, 5.8 GHz between 60 ns and 70 ns and 5.4 GHz between 70 ns and 80 ns, respectively, which are shown in Fig. 6. We also find that the chaotic oscillation frequency is enhanced by increasing the feedback level.

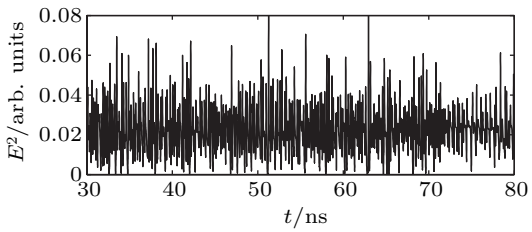



**Fig. 6.** Laser output.

### 3.3. Another road to chaos

We are also interested in bifurcation variability with other delayed time. When $\tau = 1$ ns, the result is illustrated in Figs. 7(a) and 7(b). We see clearly a quasi-periodic route to chaos with increasing the feedback levels. In the bifurcation

diagram, a stable-state ends or a bifurcation point appears at $k = 0.096$. An undamped behavior passes through the point of $k = 0.099$. The first chaotic region happens at the $k$ value between 0.102 and 0.12. With increasing the feedback levels, undamped bifurcation appears in a $k$ value range from 0.123 to 0.135. Then, quasi-periodic bifurcation appears at the $k$ value from 0.138 to 0.1608. Period-4 and period-3 are present in a $k$ value range between 0.148 and 0.155, which are illustrated in Figs. 8 and 9, respectively. An undamped behavior passes through k values from 0.1644 to 0.175. Final, the second chaotic region appears at a $k$ value higher than 0.1788.

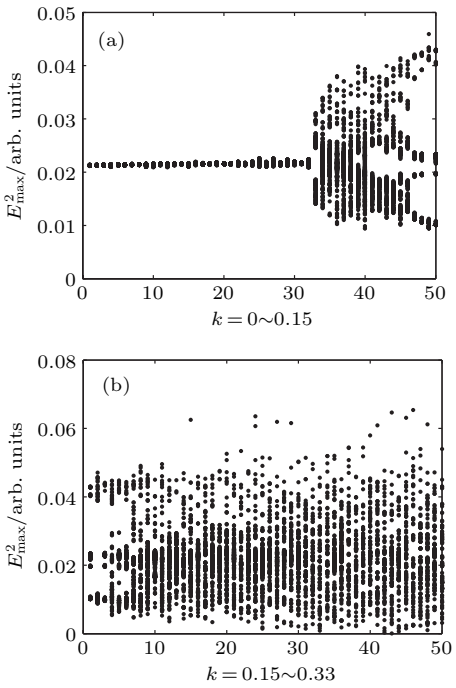



**Fig. 7.** Another bifurcation diagram with the feedback levels.

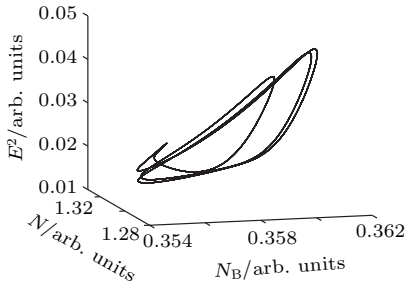



**Fig. 8.** Period-3.

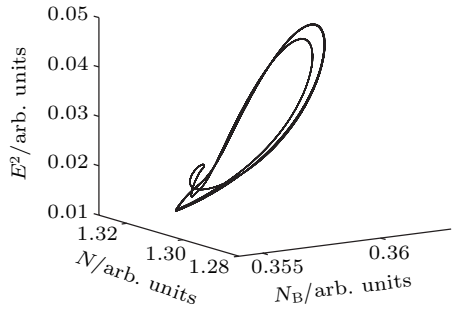



**Fig. 9.** Period-4.

### 3.4. Influence of the linewidth enhancement factor on bifurcation

The feedback level can change the population inversion and affect the complex refractive index, which will raise a shift of the laser frequency. The linewidth enhancement factor parameter usually takes a value between 3 and 8, leading to dynamic instabilities. So the linewidth enhancement factor must affect intensively the linewidth of the laser. Two roads to chaos after bifurcation are illustrated in Fig.10, where $\tau = 0.5$ ns and $k = 0.15$. To better understand the bifurcation, the value of factor $\beta_c$ is taken from 1 to 10. Figure 10 shows a stable regime in a $\beta_c$ value range between 1 and 1.9, some undamped regime from 2.08 to 2.26, a periodic regime from 2.44 to 3.88, the second undamped regime from 4.06 to 4.42 and finally the chaotic regime.

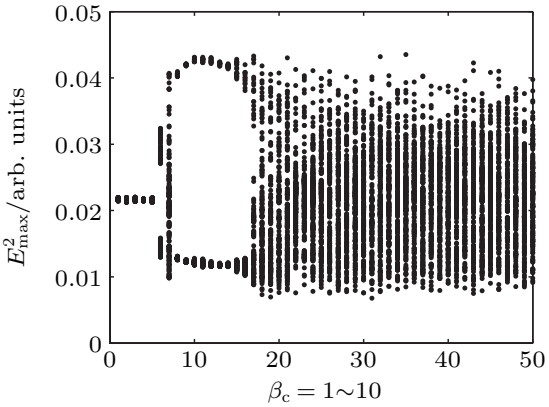



**Fig. 10.** Bifurcation diagram with linewidth enhancement factor.

### 3.5. Influence of carrier transfer on bifurcation

For MQW laser, there are the transfer of carriers from the barrier region to the well layer and the transfer of carriers escaping from the well region to the SCH layer. We find no effects of the transfer on the stability of the laser output. However, these carrier transfer behaviors can affect the dynamics of a laser. The effect of the loss of carriers transferring from the barrier region to the well layer on the dynamical behavior of the laser is more remarkable than that of the escaping rate of carriers in the SCH layer, and these two effects are opposite to each other. With the parameter values $\tau = 0.5$, $k = 0.15$ and $\gamma_{BQ}$ from $2.5 \times 10^9$/s to $2.5 \times 10^{11}$/s, figure 11 shows roughly a road to chaos after bifurcation where dynamical behavior evolves from the undamped beginning through a period to the fully developed chaos. Instead, with the parameter values $\tau = 0.5$, $k = 0.15$ and $\gamma_{QB}$ from $5 \times 10^8$/s to $2.5 \times 10^{10}$/s, figure 12 shows roughly a diversified road to stability after bifurcation where dynamical behavior of the laser evolves from the chaotic state through a period to a stable state.

With the parameter values $\tau = 1$, $k = 0.16$ and $\gamma_{BQ}$ from $1.25 \times 10^9$/s to $1.25 \times 10^{11}$/s, figure13 shows a diversified road

to chaos after quasi-periodic bifurcation and unstable oscillation with increasing the value $\gamma_{BQ}$. By adding another parameter value $\gamma_{QB}$ from $5 \times 10^8$/s to $2.5 \times 10^{10}$/s, figure 14 shows another diversified road to quasi-period and unstable oscillation after chaos. We can see that the two effects of the transfer on dynamics of the laser are contrary to each other to a certain degree.

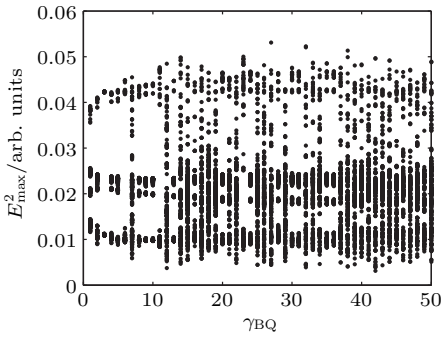



**Fig. 11.** Bifurcation diagram with loss of carriers from barrier region to well layer.

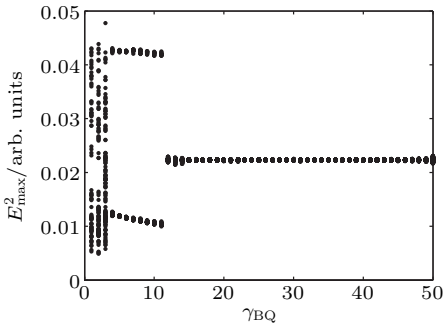



**Fig. 12.** Bifurcation diagram with loss of carriers escaping from well region to SCH layer.

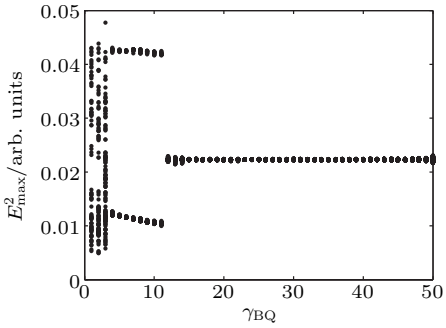



**Fig. 13.** Bifurcation diagram with loss of carriers from barrier region to well layer.

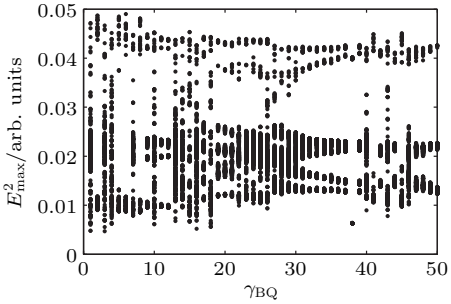



**Fig. 14.** Bifurcation diagram with loss of carriers escaping from well region to SCH layer.

### 3.6. Influence of photon loss rate on bifurcation

The photon loss rate can affect the laser behavior. Let $\tau = 0.5$, $k = 0.2$ and the photon loss rate be averagely divided into 80 intervals from $0.5 \times \gamma_p$ to $1.5 \times \gamma_p$ and figure 15 shows a road to chaos from quasi-periodic bifurcation with increasing the photon loss rate. A quasi-periodic state and unstable oscillation appear in a range lower than $0.5 \times \gamma_p$. Fully developed chaos occurs in a range higher than $0.5 \times \gamma_p$. We find that the effect of the carrier large loss rate results in the low output of laser.

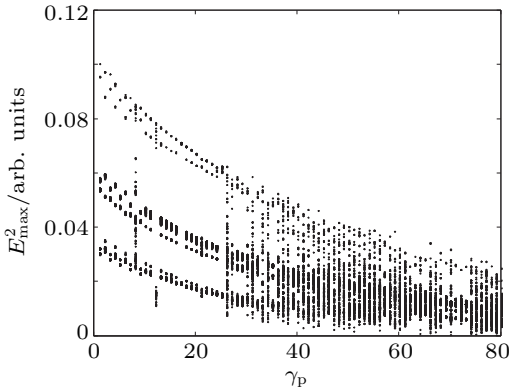



**Fig. 15.** Bifurcation diagram with photon loss rate.

### 3.7. Influence of carrier loss rate on bifurcation.

We illustrate the effect of the carrier loss rate on bifurcation behavior. Figure 15 shows mainly the effect of the carrier loss rate of parameter $A_{nr}$ on the system dynamics for $\tau = 1$ and $k = 0.2$, where the parameter $A_{nr}$ takes 0–4.5 times its value in Table 1 and is averagely divided into 80 intervals. In Fig. 16, the effect of the nonradiative recombination rate on bifurcation is conduced to quasi-period in 0–0.73125 regions. Subsequently, fully developed chaos appears in a range with $k$ being higher than 0.7875. We also find that the effects of the radiative recombination coefficient and the Auger recombination coefficient are similar to the effect of the non-radiative recombination rate on bifurcation.

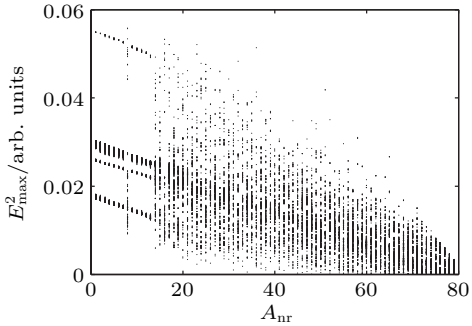



**Fig. 16.** Bifurcation diagram with nonradiative recombination rate.

### 3.8. Stable values of field in the cases of different feedback levels

We give the stable values of the field in the cases of different feedback levels to illustrate the bistable state of laser output. With $k = 0.05, 0.1, 0.15, 0.2, 0.25, 0.3, 0.35$, the values of

one output field $E$ are 0.1444, 0.1430, 0.1415, 0.1401, 0.1387, 0.1374, 0.1360, and the values of another output field $E$ are 0.1460, 0.1461, 0.1463, 0.1465, 0.1466 and 0.1468, 0.1469. This result conforms to our prediction of the bistable state.

## 4. Conclusions

We have analyzed theoretically the unmoving point to predict the bistable state of the laser. We find that the gain shifts abruptly. Using a linear stability analysis method and the characteristic equation, we predict the stability of the system and make several approximate analyses of the stability of the equilibrium point, and we also discuss the quantitative criteria of bifurcation. We give a formula for the relaxation oscillation frequency of the laser. The relaxation frequency is demonstrated to be a function of the laser parameters, the feedback level and delayed time. We reveal two relaxation oscillation frequencies for the periodic laser and find multi-frequency characteristics for the chaotic laser. We illustrate a road to chaos from a stable state to quasi-periodic states with feedback level increasing. The effects of the transfers of carriers on dynamic behaviors are analyzed via the bifurcation diagram. The above two effects on laser dynamics are contrary to each other. We show other roads to chaos after bifurcation by changing the linewidth enhancement factor, the photon loss rate and the carrier loss rate separately. The transfers of carriers can change remarkably the laser dynamics. These results are referred to the studies of MQW laser, complex system and laser physics and their applications.

## References


[1] Mørk J, Tromborg B and Mark J 1992 *IEEE J. Quantum Electron.* **28** 93
[2] Kirk G and Bernd K 2004 *Opt. Commun.* **231** 383
[3] Jones R J, Spencer P S, Lawrence J and Kane D M 2001 *IEE Proc. Optoelectron.* **148** 7
[4] Yan S L 2009 *J. Mod. Opt.* **56** 539
[5] Sunada S, Harayama T, Arai K, Yoshimura K, Davis P, Tsuzuki K and Uchida S 2011 *Opt. Express* **19** 5713
[6] Wu L and Zhu S Q 2003 *Chin. Phys.* **12** 300
[7] Yan S L 2007 *Chin. Phys.* **16** 3271
[8] Argyris A, Syvridis D, Larger L, Annovazzi-Lodi V, Colet P, Fischer I, García-Ojalvo J, Mirasso C R, Pesquera L and Shore K A 2005 *Nature* **438** 343
[9] Argyris A, Grivas E, Hamacher M, Bogris A and Syvridis D 2010 *Opt. Express* **18** 5188
[10] Houlihan J, Huyet G and Mcinerney J G 2001 *Opt. Commun.* **199** 175
[11] Mandel P, Viktorov E A, Masoller C and Torre M S 2003 *Physica A* **327** 129
[12] Yan S L 2009 *Opt. Commun.* **282** 3558
[13] Sivaprakasam S, Pierce I, Rees P, Spencer P S, Heil K A T, Fischer I, Elsasser W and Gavrielides A 2001 *Phys. Rev. Lett.* **87** 243
[14] Li X F, Pan W, Luo B, Ma D and Deng G 2006 *Proc. Inst. Electr. Eng. Optoelectron.* **153** 67
[15] Wang A B, Wang Y C and He H C 2008 *IEEE Photon. Technol. Lett.* **20** 1633
[16] Ju R and Spencer P S 2005 *J. Lightwave Technol.* **23** 2513
[17] Murakami A and Ohtsubo J 1998 *IEEE J. Quantum Electron.* **34** 1979
[18] Xiang S Y, Pan W, Yan L, Luo B, Zou X, Jiang N and Wen K 2011 *Opt. Lett.* **36** 310
[19] Yan S L 2012 *Opt. Laser Technol.* **44** 83
[20] Wu J G, Zhao L J, Wu Z M, Lu D, Tang X, Zhong Z Q and Xia G Q 2013 *Opt. Express* **21** 23358
[21] Xiang S, Pan W, Zhang L, Wen A, Shang L, Zhang H and Lin L 2014 *Opt. Commun.* **324** 38
[22] Yan S L 2015 *Acta Phys. Sin.* **64** 240505 (in Chinese)
[23] Liu Q X, Pan W, Zhang L Y, Li N Q and Yan J 2015 *Acta Phys. Sin.* **64** 024209 (in Chinese)
[24] Wang S T, Wu Z M, Wu J G, Zhou L and Xia G Q 2015 *Acta Phys. Sin.* **64** 154205 (in Chinese)
[25] Yan S L 2016 *Chin. Phys. B* **25** 090504
[26] Sunada S, Shinohara S, Fukushima T and Harayama T 2016 *Phys. Rev. Lett.* **116** 203903
[27] Naruse M, Terashima Y, Uchid A and Kim S J 2017 www.nature.com/scientificreports/ DOI: 10.1038/s41598-017-08585-8, pp. 1–10
[28] Wang A B, Wang Y C and Wang J F 2009 *Opt. Lett.* **34** 1144
[29] Wang A B, Yang Y B, Wang B J, Zhang B B, Li L and Wang Y C 2013 *Opt. Express* **21** 8701
[30] Bennett S, Snowden C M and Iezekiel S 1997 *IEEE J. Quantum Electron.* **33** 2076